Ionic Thermoplastic Elastomer Based on the Zinc Salt of Sulfonated Maleated EPDM Rubber. II. Reinforcement by Fillers

SWAPAN K. GHOSH, P. P. DE, D. KHASTGIR, S. K. DE

Rubber Technology Centre, Indian Institute of Technology, Kharagpur-721302, India

Received 23 July 1999; accepted 10 January 2000

ABSTRACT: Incorporation of SRF and ISAF grades of carbon black and precipitated silica improves the physical properties of the zinc stearate plasticized ionomer, namely, the zinc salt of sulfonated maleated EPDM rubber, which behaves as an ionic thermoplastic elastomer. The reinforcing ability of the fillers follows the order SRF carbon black < silica < ISAF carbon black. The activation energy of the melt flow also follows the same order. The results of infrared spectroscopic studies and dynamic mechanical studies reveal that, apart from the rubber–filler bonding, as is normally observable in diene rubbers, ion–dipole and hydrogen-bonding interactions occur between the active sites on the filler surface and the ionic aggregates. © 2000 John Wiley & Sons, Inc. J Appl Polym Sci 78: 326–337, 2000

Key words: fillers; processability; dynamic mechanical thermal analysis; infrared spectroscopy; reprocessability; physical properties

INTRODUCTION

Reinforcing fillers are generally known to adversely affect the physical properties of thermoplastic elastomers.[1] However, in the case of ionic thermoplastic elastomers, reinforcing carbon black and precipitated silica fillers are reported to improve the properties.[2–7] The previous communication reports the effect of zinc stearate on the properties of an ionic elastomer, namely, zinc salt of sulfonated maleated EPDM rubber (Zn-s-m-EPDM).[8] The present article reports the results of studies on the effects of fillers, namely, precipitated silica, semireinforcing furnace (SRF), and intermediate super abrasion furnace (ISAF) blacks on the rheological and physicomechanical properties of zinc stearate-filled Zn-s-m-EPDM.

Correspondence to: S. K. De.

Contract grant sponsor: Council of Scientific and Industrial Research (CSIR), Government of India, New Delhi.

Journal of Applied Polymer Science, Vol. 78, 326–337 (2000)

EXPERIMENTAL

Materials

Polymer

Preparation of the sulfonated maleated EPDM and its zinc salt were discussed in earlier communications.[8,9] Zn-s-m-EPDM containing 30 phr of zinc stearate was used in the present study. Details of the materials used are provided in the previous communication.[8]

Fillers

ISAF Black. ISAF black was obtained from Degussa AG (Frankfurt, Germany). The characteristics were as follows: nitrogen surface area, 105 m^2/g; pH 9.5; and wt % of O_2, 0.9.

SRF Black. SRF black was supplied by Philips Carbon Black Ltd. (Durgapur, India). The characteristics were as follows: nitrogen surface area, 20 m^2/g; pH 7.5; and wt % of O_2, 0.2.

Precipitated Silica. Precipitated silica filler of grade Ultrasil VN3 was obtained from Degussa AG. Its characteristics were as follows: specific gravity, 2.20 gm/cc; nitrogen surface area, 234 m^2/g; and pH 6.0.

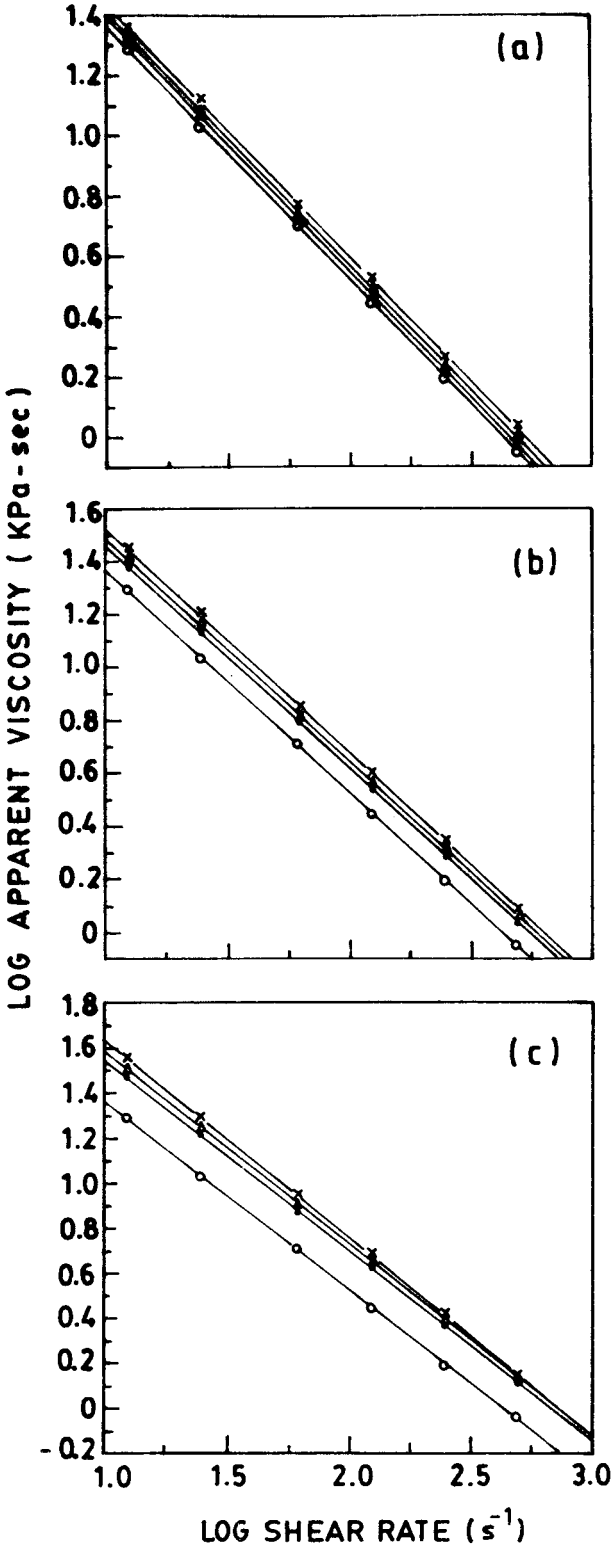

Figure 1 Plots of log apparent viscosity (η) versus log apparent shear rate (s^{-1}) for Zn-s-m-EPDM in the presence of (—○—) 30 phr zinc stearate, and (a) (—●—) 10 phr, (—△—) 20 phr, and (—x—) 30 phr SRF black-filled systems; (b) (—●—) 10 phr, (—△—) 20 phr, and (—x—) 30 phr silica-filled systems; and (c) (—●—) 10 phr, (—△—) 20 phr, and (—x—) 30 phr ISAF black-filled systems.

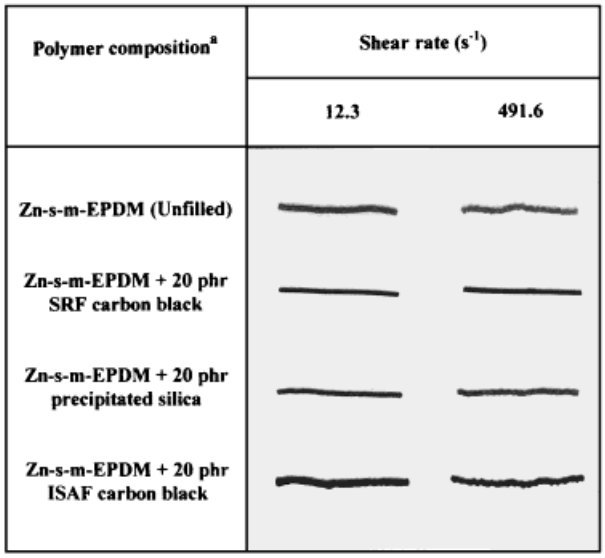

Figure 2 Photomicrographs of representative extrudates at 190°C and at different shear rates.

Sample Preparation

The carboxylated–sulfonated ionomer filled with 30 phr of zinc stearate was mixed with the filler in a two-roll mill with a tight nip to form smooth bands. Mixing was done at room temperature and cold water was circulated through the rolls to prevent an excessive temperature increase during mixing.

Test Methods

The experimental techniques for measurements of the processability behavior, physical properties, dynamic mechanical, and infrared spectroscopic studies were discussed in the previous communication.[8]

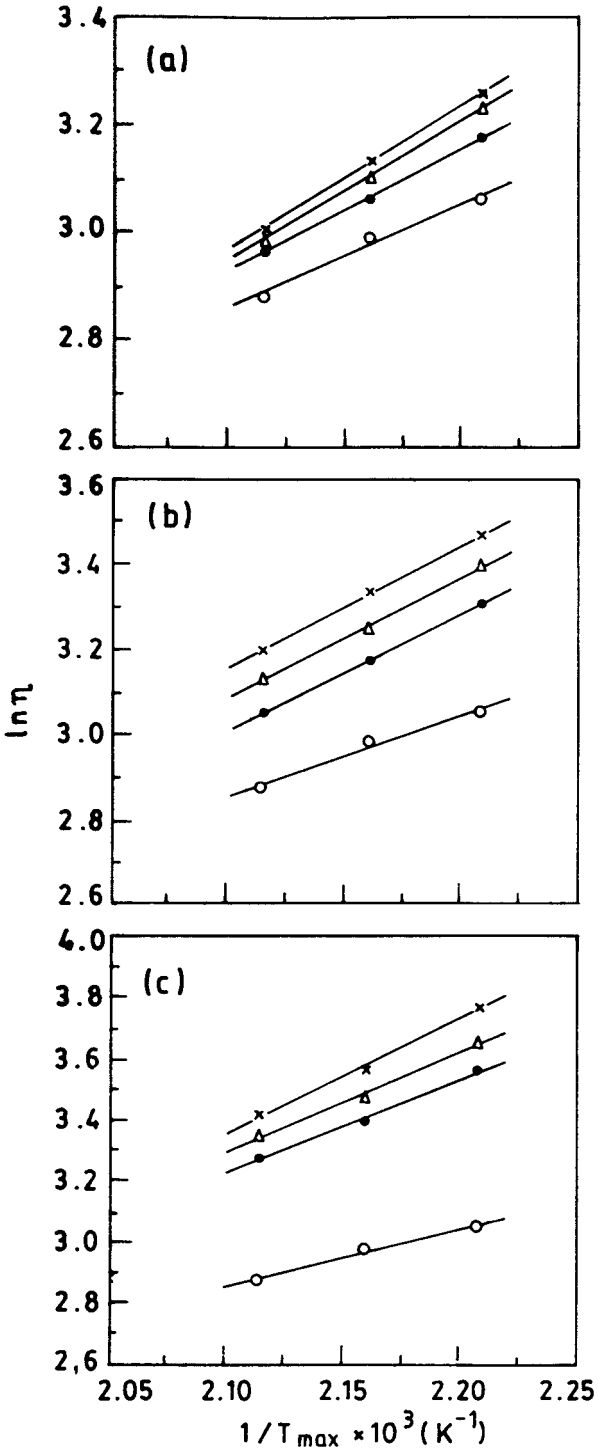

Figure 3 Arrehenius plots showing variation of ln apparent viscosity (η) versus $1/T_{max}$ for Zn-s-m-EPDM in the presence of (—○—) 30 phr zinc stearate, and (a) (—●—) 10 phr, (—△—) 20 phr, and (—x—) 30 phr SRF black-filled systems; (b) (—●—) 10 phr, (—△—) 20 phr, and (—x—) 30 phr silica-filled systems; and (c) (—●—) 10 phr, (—△—) 20 phr, and (—x—) 30 phr ISAF black-filled systems.

Table I Activation Energy for Viscous Flow in kJ/mol

Polymer Composition[a]	Filler Loading (phr)[b]	Shear Rate (s^{-1}) 12.3	491.6
Zn-s-m-EPDM (unfilled)	—	15.9	12.1
Zn-s-m-EPDM + SRF carbon black	10	19.1	15.5
	20	21.9	18.4
	30	22.6	18.8
Zn-s-m-EPDM + precipitated silica	10	22.9	17.9
	20	23.3	18.7
	30	23.9	19.2
Zn-s-m-EPDM + ISAF carbon black	10	25.7	22.7
	20	27.5	25.2
	30	31.3	28.1

[a] All compositions contain 30 phr zinc stearate.
[b] phr stands for parts per 100 parts of rubber (by weight).

Scanning Electron Microscopic Studies

Scanning electron micrographs of the tensile fractured surfaces of the polymers were taken with a scanning electron microscope (Hitachi, Model S-415A, Japan). The accelerating voltage was 25 kV.

RESULTS AND DISCUSSION

Processability Studies

Figure 1 shows log–log plots of the apparent viscosity versus the apparent shear rate at 190°C for the different ionomeric compositions. It is evident from the figure that the materials behave as pseudoplastic fluids. The viscosity decreases with increase in the shear rate, but the difference in viscosity between low (12.3 s^{-1}) and high (491.6 s^{-1}) shear rates increases with increase in the reinforcing ability of the fillers (i.e., gum < SRF black < silica < ISAF black). This indicates that incorporation of a filler makes the ionomer more shear sensitive due to ionic cluster–filler interactions.[2–7] Incorporation of fillers increases the melt viscosity

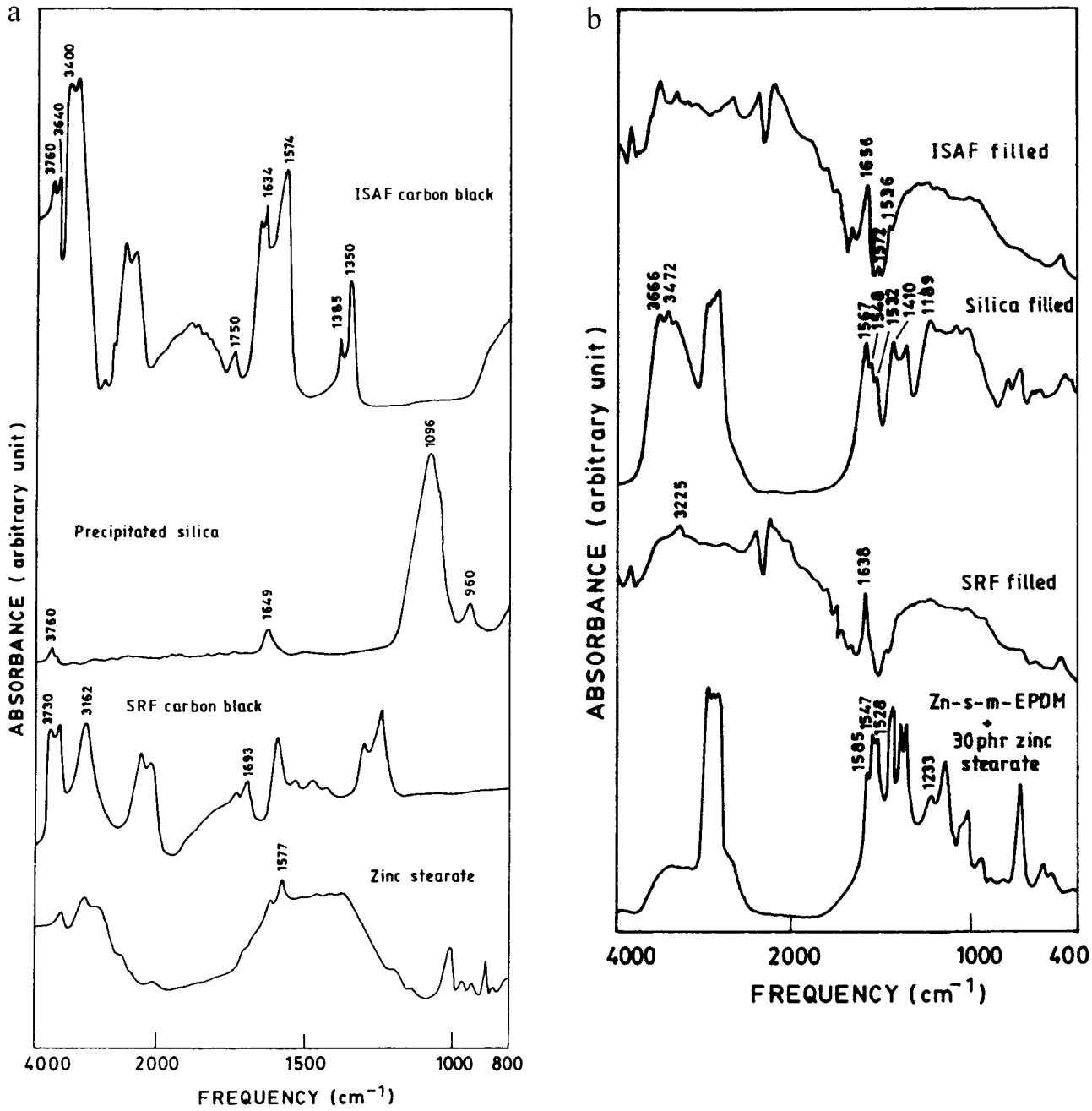

Figure 4 (a) Infrared spectra of zinc stearate, SRF carbon black, silica, and ISAF carbon black. (b) Infrared spectra of Zn-s-m-EPDM containing zinc stearate, SRF carbon black, silica, and ISAF carbon black.

which follows the order SRF black < silica < ISAF black. As discussed later, the reinforcing ability of the fillers also follows the same order. Active sites of both carbon black and silica particles are known to interact with the ionic aggregates of ionomers in the region of the restricted mobility of the polymer segments, apart from the conventional rubber–filler bonding occurring in the free mobility region of the polymer segments.[4–7]

Photomicrographs of the extrudates at different shear rates are shown in Figure 2. While the SRF black-filled system shows no melt fracture at any shear rate, the precipitated silica-filled sys-

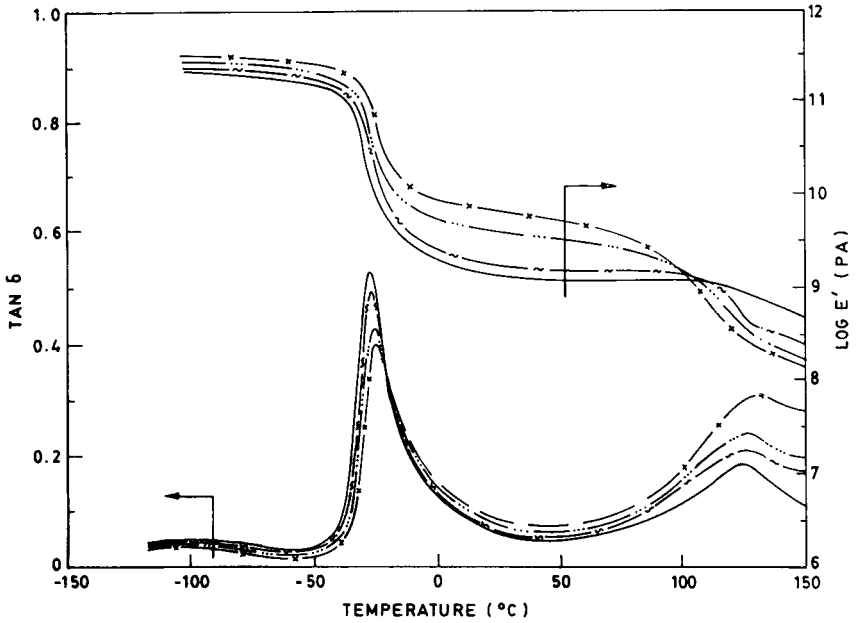

Figure 5 Plots of tan δ and log E' versus temperature for (—) Zn-s-m-EPDM + 30 phr zinc stearate, (—~—) Zn-s-m-EPDM + 30 phr zinc stearate + 20 phr SRF black, (— · · · —) Zn-s-m-EPDM + 30 phr zinc stearate + 20 phr silica, and (—x—) Zn-s-m-EPDM + 30 phr zinc stearate + 20 phr ISAF black.

tem shows melt fracture at higher shear rates and the ISAF black-filled system shows melt fracture at all shear rates.

Expectedly, viscosity decreases with increase in temperature. The activation energy for the melt flow, which is shear-rate-dependent, was calculated on the basis of the Arrhenius equation[10]:

$$\eta = Ae^{E/RT} \quad (1)$$

where η is the apparent viscosity at a temperature T (K); A, the frequency factor; E, the activation energy for the melt flow; and R, the universal gas constant. Activation energy was calculated from the plots of ln η versus $1/T$ (Fig. 3) and the results are summarized in Table I. Incorporation of a filler increases the activation energy for the melt flow, which follows the order gum < SRF black < silica < ISAF black. In all systems, an increase in shear rate causes a decrease in shear-

Table II Results of Dynamic Mechanical Thermal Analyses

Polymer Composition[a]	T_g (°C)	tan δ at T_g	T_i (°C)	tan δ at T_i	Storage Modulus (Pascal) × 10^8 25°C	140°C
Zn-s-m-EPDM (unfilled)	−26.1	0.52	123.8	0.18	13.1	5.6
Zn-s-m-EPDM + 20 phr SRF carbon black	−25.8	0.50	124.7	0.21	16.3	2.9
Zn-s-m-EPDM + 20 phr precipitated silica	−25.6	0.43	127.2	0.24	35.5	2.0
Zn-s-m-EPDM + 20 phr ISAF carbon black	−24.0	0.40	132.4	0.30	60.0	1.7

[a] All compositions contain 30 phr zinc stearate.

rate-dependent activation energy for the melt flow.

Infrared Spectroscopic Studies

Infrared spectra of zinc stearate, precipitated silica, and SRF and ISAF grades of carbon black are shown in Figure 4(a). Zinc stearate shows the characteristic absorbance at 1577 cm^{-1} which is believed to be due to the asymmetric stretching of the bridging type of carboxylate groups.[11] The spectra of precipitated silica are characterized by the strong absorbance at 1096 cm^{-1} which is due to Si—O—Si asymmetric stretching. The other characteristic peaks at 3760, 960, and 798 cm^{-1} are due to —OH stretching of Si—OH, Si—O stretching of Si—OH, and Si—OH deformation, while the peak at 470 cm^{-1} is due to Si—O—Si symmetric stretching.[12] SRF carbon black shows the characteristic absorbance at 3730 cm^{-1} which is due to O—H groups in the substituted phenolic compounds.[13] The broad peak at 3162 cm^{-1} is attributed to composite absorption of hydrogen-bonded —OH groups from alcohol, phenols, and enols.[14] The peak at 1693 cm^{-1} is believed to be due to a carbonyl stretching vibration. ISAF carbon black shows absorbance bands at 1350 and 1385 cm^{-1} which are due to —OH bending in water and C—O stretching in phenols.[11] The band at 1574 cm^{-1} confirms the presence of tetrahydroquinone, whereas the peak around 1634 cm^{-1} is due to polycyclic quinones.[13,14] The absorbance band at 1750 cm^{-1} confirms the presence of lactones and a broad band at 3400 cm^{-1} is due to hydrogen-bonded phenolic O—H groups, while the other two bands at 3640 and 3760 cm^{-1} occur due to free O—H stretching of adsorbed water and phenols.[14] The infrared spectra of a zinc stearate-filled ionomer were discussed in the previous communication.

Figure 4(b) shows that the infrared spectra of the filler-loaded ionomers are different from the corresponding neat ionomer and the filler. In the case of the silica-filled ionomer, the peak at 3472 cm^{-1} is believed to be due to the hydrogen-bonded structure in the vicinal silanol groups and the peak at 3666 cm^{-1} is ascribed to the hydrogen-bonded structure involving silanol groups and carboxylate anions.[15] The peak in the asymmetric stretching region occurs at 1567, 1548, and 1532 cm^{-1} and the carboxylate symmetric stretching occurs at 1410 cm^{-1}. The peak at 1189 cm^{-1} is due to the asymmetric stretching of the sulfonate groups. The split pattern between 1000 and 1200

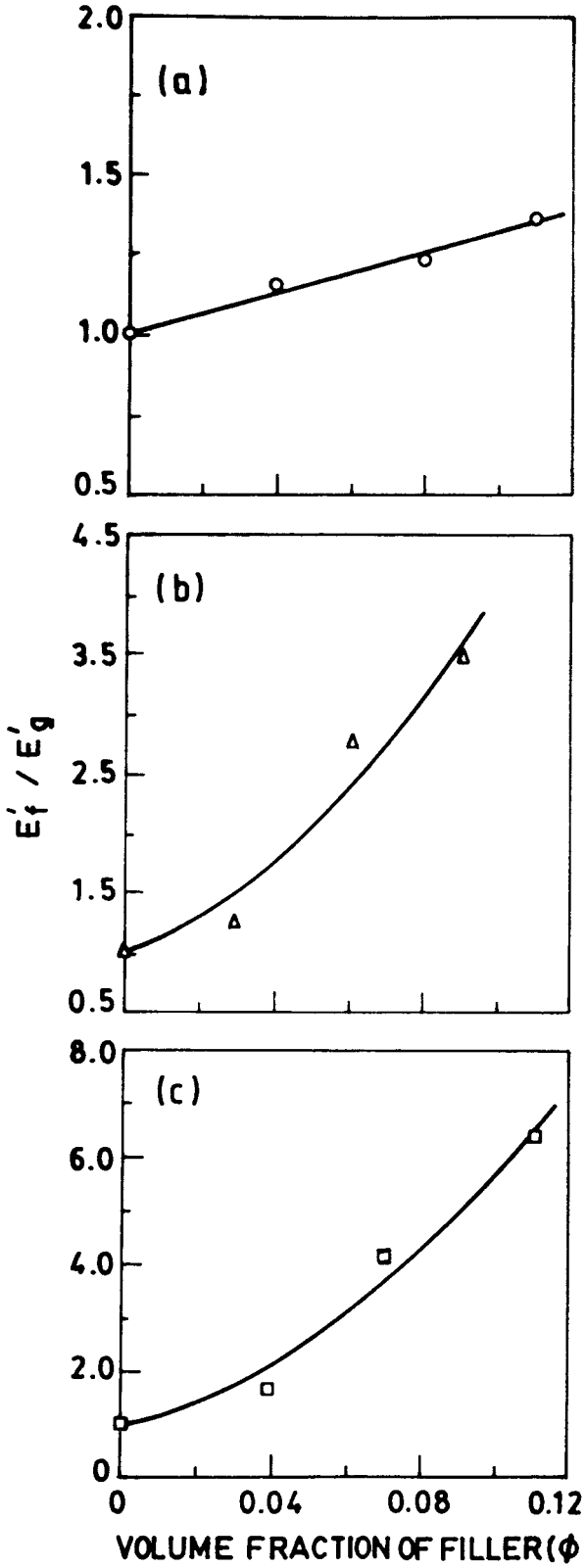

Figure 6 Variation of E'_f/E'_g against volume fraction of filler (ϕ) at room temperature (25°C) for (—○—) SRF, (—△—) silica-, and (—□—) ISAF-filled ionomer.

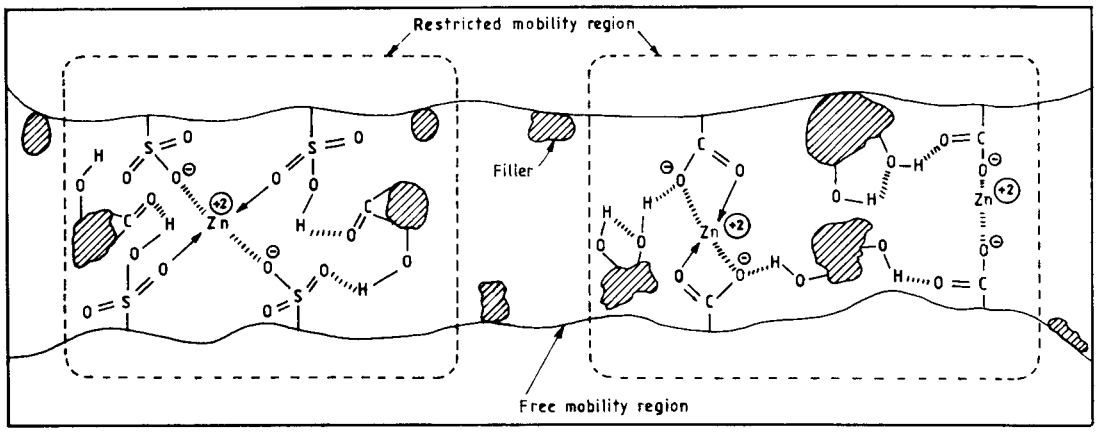

Figure 7 Proposed schematic representation showing interactions between the filler surface and the ionomer.

cm^{-1} indicates specific interaction of the silica filler with the sulfonate group. The ionomeric compositions filled with SRF and ISAF grades of carbon blacks show a broad band in the sulfonate stretching frequency region (800–1400 cm^{-1}). Furthermore, the SRF carbon black-filled ionomer shows a broad band at 3225 cm^{-1} which is believed to be due to a composite absorption by the hydrogen-bonded O—H groups present in both carbon black and the ionomer.[11,13] It also shows an absorbance peak at 1638 cm^{-1} which is due to hydrogen-bonded carbonyl groups. The ISAF carbon black-filled ionomer shows band splitting in the high-frequency region. It shows the presence of a carbonyl stretching frequency at 1656 cm^{-1} and the presence of 1572 and 1536 cm^{-1} peaks arising out of the hydrogen-bonded carboxylate anions.[14,16] The filler-loaded ionomer contains band splitting at the carboxylate and sulfonated stretching frequency regions, thereby confirming an interaction between the active sites of the filler and the zinc stearate-filled ionomer.

Dynamic Mechanical Thermal Analysis

Figure 5 shows the effect of fillers on the dynamic mechanical properties of the zinc stearate-filled ionomer. The results of dynamic mechanical properties are summarized in Table II. Apart from the glass–rubber transition (the corresponding temperature abbreviated as T_g), a high temperature transition known as the ionic transition occurs (the corresponding temperature abbreviated as T_i), which is due to the relaxation of the restricted mobility region attached to the ionic aggregates.[17] As the reinforcing ability of the filler increases, T_i shifts to higher temperature and the peak height (tan δ) at T_i increases along with broadening of the peak. The magnitude of increase in tan δ at T_i as well as of shifting of T_i toward higher temperature follows the order gum < SRF black < silica < ISAF black. It is also observed that, depending on its reinforcing ability, incorporation of a filler causes marginal shifting of the T_g toward higher temperature and lowering of tan δ at T_g, which is ascribed to the rubber–filler bonding, as is normally observable in the case of diene rubbers.[18,19] It is believed that filler particles interact with both the main-chain segments (free mobility regions) away from the ionic aggregates and the restricted mobility regions of the chain segments around the clusters of the ionic aggregates. Similar observations were made by Datta et al. in the case of zinc salt of maleated EPDM,[6,7] by Kurian et al. in the case of zinc salt of sulfonated EPDM,[3,5] and by Mondal et al. in the case of zinc salt of carboxylated nitrile rubber.[4] From Figure 5, it is also evident that at ambient temperature E' increases in the order gum < SRF black < silica < ISAF black. However, at higher temperature (140°C), E' follows the reverse order. This is due to the melting of zinc stearate and the subsequent plasticization of the ionic rubber by zinc stearate. It is observed that plasticization of the polymer in the presence of fillers occur at a lower temperature, and the higher the reinforc-

ing ability of the filler, the greater is the rate of fall of the modulus at elevated temperature (>100°C). The dependence of the room-temperature storage modulus on filler loading is shown in Figure 6. The results could be fitted by the following equations:

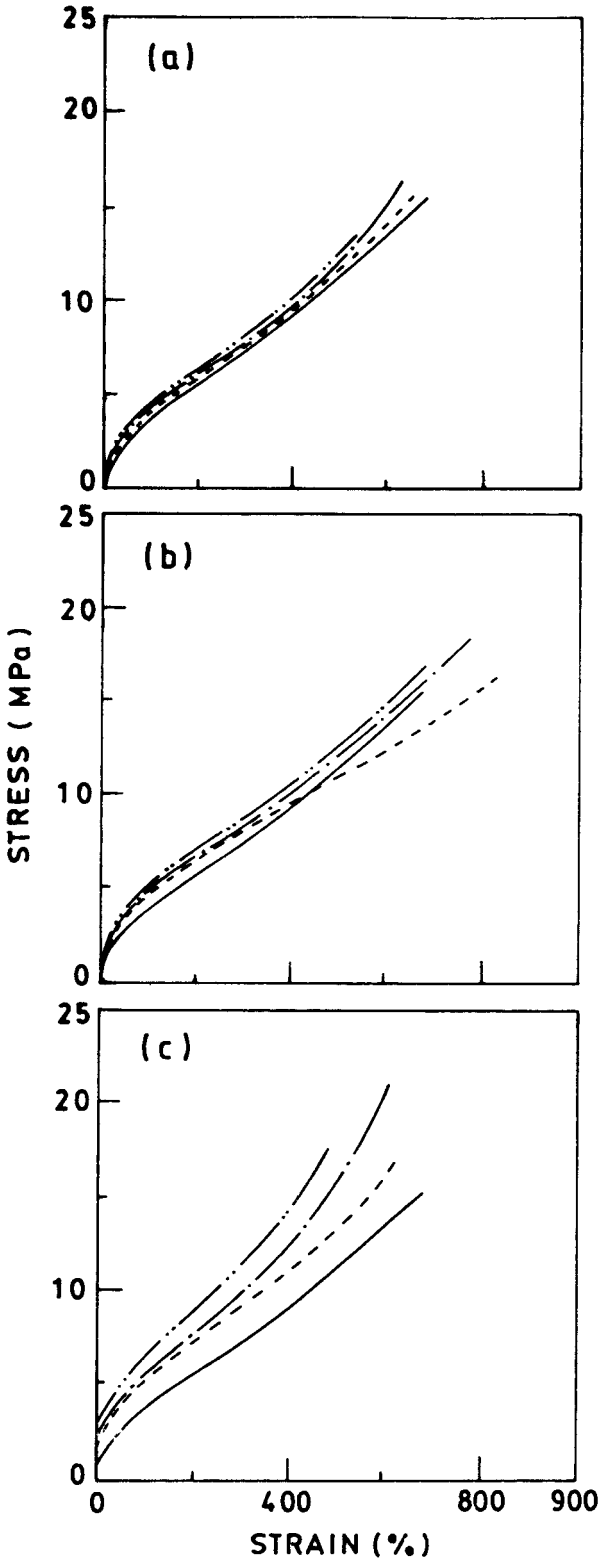

(a) for SRF black: $E'_f/E'_g = 1.0 + 3.1\phi$, (2)

(b) for silica: $E'_f/E'_g = 1.0 + 17\phi + 142\phi^2$, (3)

(c) for ISAF black: $E'_f/E'_g = 1.0 + 29\phi + 221\phi^2$ (4)

where E_f is the storage modulus of the filled system and E_g refers to the modulus of the unfilled system and ϕ is the volume fraction of the filler. These equations are very similar to the relationships proposed by Smallwood in the case of diene rubbers.[20] The greater the slope, the stronger is the rubber–filler bonding. In the case of highly reinforcing fillers, the plots deviate from linearity. On the basis of the above discussion, a schematic diagram showing rubber–filler attachments in both free mobility and restricted mobility regions of the polymer segments is presented in Figure 7.

Physical Properties

The stress–strain plots of the polymers at room temperature are shown in Figure 8 and the physical properties are listed in Table III. It is evident that incorporation of the filler causes an increase in the modulus, hardness, and tensile and tear strength and the reinforcing ability follows the order SRF carbon black < silica < ISAF carbon black. While carbon blacks cause a decrease in the elongation at break, the increase in the elongation at break on silica incorporation is believed to be due to slippage of the polymer chains over the silica surface.[21] For the three fillers studied, 20 phr of filler loading is found to be optimum, beyond which physical properties decrease. Incorporation of the filler increases the tension set marginally, which is believed to be due to ionic interchanges (ion

Figure 8 Stress–strain plots of (—) Zn-s-m-EPDM + 30 phr Znst. and (a) (— — —) 10 phr, (— · —) 20 phr, and (— · · —) 30 phr SRF black-filled systems; (b) (— — —) 10 phr, (— · —) 20 phr, and (— · · —) 30 phr silica-filled systems; and (c) (— — —) 10 phr, (— · —) 20 phr, and (— · · —) 30 phr ISAF black-filled systems.

Table III Physical Properties

Polymer Composition[a]	Filler Loading (phr)	Modulus (MPa) at an Elongation of 100%	Modulus (MPa) at an Elongation of 300%	Tensile Strength (MPa)	Elongation at Break (%)	Tear Strength (kNm^{-1})	Tension Set at 100% Elongation (%)	Hardness (Shore A)
Zn-s-m-EPDM (unfilled)	—	3.8	7.3	15.4	690	63	14	63
Zn-s-m-EPDM + SRF carbon black	10	4.3	7.6	15.8	660	65	14	69
	20	4.5	7.9	16.6	641	66	16	72
	30	4.8	8.2	13.5	534	68	16	74
Zn-s-m-EPDM + precipitated silica	10	4.5	7.9	16.2	837	64	17	71
	20	4.8	8.2	18.4	789	65	19	73
	30	5.1	8.6	16.9	688	67	20	74
Zn-s-m-EPDM + ISAF carbon black	10	5.2	9.3	17.1	632	70	18	73
	20	5.7	10.0	21.4	616	73	19	77
	30	6.4	11.7	17.4	483	75	22	80

[a] All compositions contain 30 phr zinc stearate.

hopping) and slippage of the polymer chains over the filler surface.

Figure 9 shows plots of E_f/E_g versus the volume fraction of the filler at room temperature. Here, E refers to the static modulus at 25% elongation and f and g stand for the filled and gum systems. The results could be fitted by the following equations:

$$\text{(a) for SRF black: } E_f/E_g = 1 + 3.9\phi, \quad (5)$$

$$\text{(b) for silica: } E_f/E_g = 1 + 5.9\phi, \quad (6)$$

$$\text{(c) for ISAF black: } E_f/E_g = 1 + 10.1\phi \quad (7)$$

It is evident that the magnitude of the slope represents the extent of the interaction between the polymer and the filler, which follows the order gum < SRF carbon black < silica < ISAF carbon black.

Scanning Electron Microscopic Studies

Representative scanning electron micrographs of tensile fracture surfaces of the polymers are shown in Figure 10. Figure 10(a) shows a network of channel-type cracks with a large number of smaller tear lines on the cracked surfaces which is similar to EPDM vulcanizates.[22] Addition of zinc stearate to the system increases the strength and changes the fractograph remarkably. The network of cracks is overshadowed by the roughness of the surface. Although the tensile strength is not improved significantly by incorporation of SRF carbon black, the fracture surface shows a different pattern with brittle fracture.[23] With the addition of silica filler, the strength of the ionomer increases remarkably, and the surface is rough with large-sized cracked surfaces. A rough surface and a network of small-sized cracks are the features of the ISAF carbon black-filled system, which also registers the maximum tensile strength. The fractographs are similar to fractured surfaces of conventional rubber reinforced by fillers.[24] Strong rubber–filler attachments prevent the fracture path from proceeding straight and is manifested in the roughness of the fracture surface with a network of cracks.[25]

Reprocessability Studies

Figure 11 shows the dependence of the apparent viscosity and tensile strength of the extrudates of

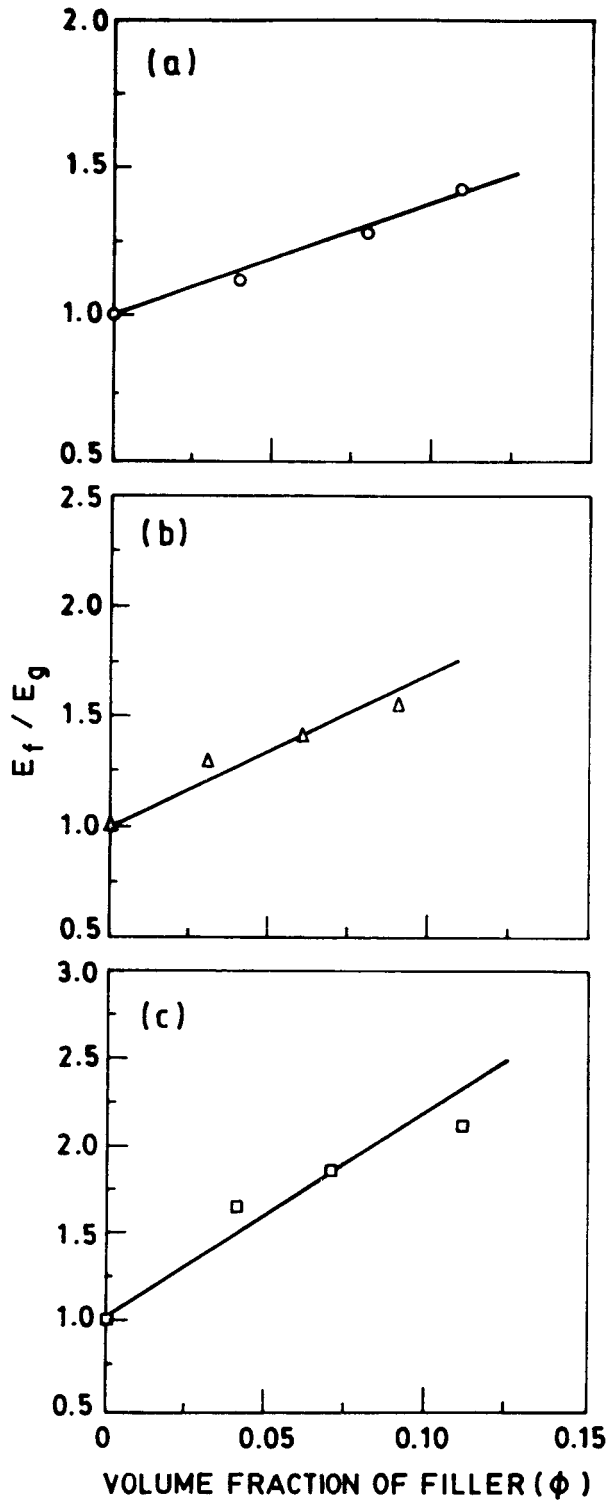

Figure 9 Variation of E_f/E_g at 25% elongation against volume fraction of filler (ϕ) at room temperature (25°C) for (—○—) SRF black, (—△—) silica-, and (—□—) ISAF black-filled ionomer.

the plasticized ionomer, filled with different fillers, on the number of cycles of extrusion through a Monsanto processability tester (MPT). It is observed that the viscosity of the polymers and the tensile strength of the extrudates remain almost constant upon repeated extrusions. This shows that the zinc stearate-plasticized ionomers in the presence of fillers behaves as a thermoplastic elastomer and can be reprocessed without deterioration in the properties.

CONCLUSIONS

1. A zinc stearate-plasticized ionomer, namely, zinc salt of sulfonated maleated EPDM rubber, can be reinforced by fillers and the reinforcing ability follows the order SRF carbon black < precipitated silica < ISAF carbon black. Fillers increase the hardness, modulus, tensile strength, tear resistance, and tension set. Elongation at break for carbon black-filled systems decreases, while the same for the silica-filled system increases.
2. Infrared spectroscopic studies indicate the occurrence of ion–dipole and hydrogen-bonding type of interactions between active sites on the filler surface and the ionic groups of the polymer.
3. Dynamic mechanical thermal analyses revealed that the rubber–filler bonding in the present case is of two types: first, interaction between the filler particles and the backbone chains in the free mobility regions, which is similar to the interaction involving diene rubbers and reinforcing fillers. This is manifested in lowering of tan δ at the glass–rubber transition temperature (T_g), and second, interaction between the ionic aggregates in the restricted mobility regions of the chain segments and the filler particles, which is manifested in an increase in tan δ at T_i, referred to as the temperature for ionic transition occurring at elevated temperature.
4. The ionomer plasticized by zinc stearate and reinforced by fillers exhibits a thermoplastic flow behavior.

The authors gratefully acknowledge the financial assistance from the Council of Scientific and Industrial Research (CSIR), Government of India, New Delhi.

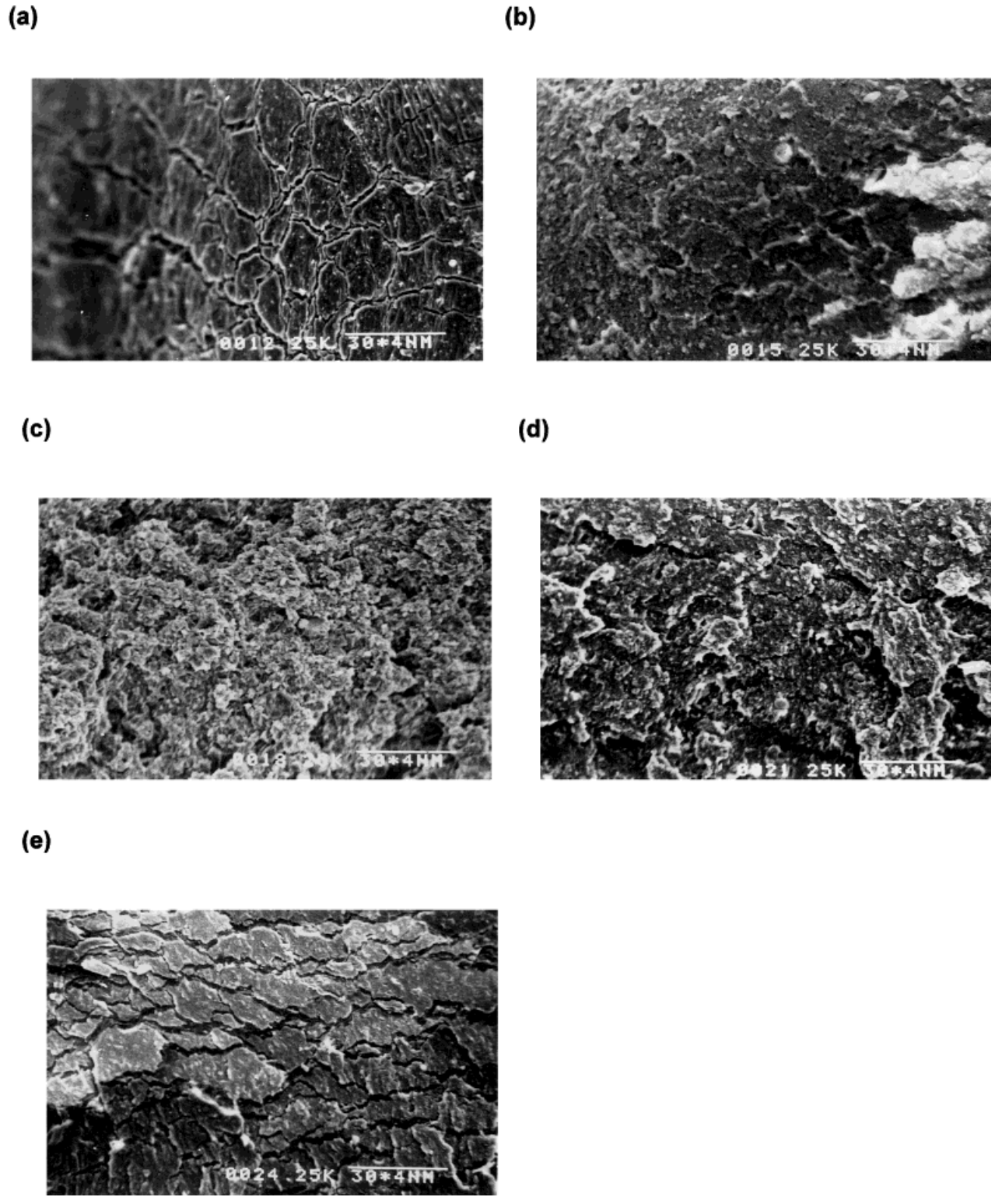

Figure 10 Tensile fractographs of (a) Zn-s-m-EPDM, (b) Zn-s-m-EPDM + 30 phr zinc stearate, (c) Zn-s-m-EPDM + 30 phr zinc stearate + 20 phr SRF carbon black, (d) Zn-s-m-EPDM + 30 phr zinc stearate + 20 phr silica and (e) Zn-s-m-EPDM + 30 phr zinc stearate + 20 phr ISAF carbon black.

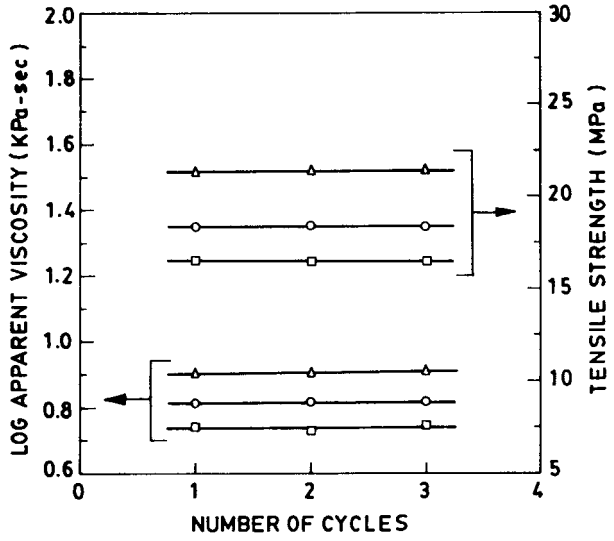

Figure 11 Plots of log apparent viscosity (η) and tensile strength versus number of cycles of extrusion for (—□—) SRF carbon black-, (—○—) silica-, and (—△—) ISAF carbon black-filled systems.

REFERENCES

1. Quan, E. J. In Handbook of Fillers and Reinforcements for Plastics; Katz, H. S.; Milewski, J. V., Eds.; Van Nostrand Reinhold: New York, 1978; Chapter 6.
2. Sato, K. Rubb Chem Technol 1993, 56, 942.
3. Kurian, T.; De, P. P.; Khastgir, D.; Tripathy, D. K.; Peiffer, D. G.; De, S. K. Polymer 1995, 36, 3875.
4. Mondal, U. K.; Tripathy, D. K.; De, S. K. Polymer 1993, 18, 3833.
5. Kurian, T.; De, P. P.; Tripathy, D. K.; Peiffer, D. G.; De, S. K. Polymer 1996, 24, 5597.
6. Datta, S.; Bhattacharya, A. K.; De, S. K.; Kontos, E. G.; Wefer, J. M. Polymer 1996, 37, 2581.
7. Datta, S.; De, S. K.; Kontos, E. G.; Wefer, J. M.; Vidal, A. Polymer 1996, 37, 3431.
8. Ghosh, S. K.; De, P. P.; Khastgir, D.; De, S. K. J Appl Polym Sci, in press.
9. Ghosh, S. K.; De, P. P.; Khastgir, D.; De, S. K. Polym Plast Technol Eng 2000, 39, 47.
10. Tager, A. Physical Properties of Polymers; Mir: Moscow, 1980.
11. Socrates, G. Infrared Characteristic Group Frequencies; Wiley-Interscience: Chichester, 1980.
12. Willams, D. H.; Flemming, I. Spectroscopic Methods in Organic Chemistry; McGraw-Hill: New York, 1987.
13. Donnet, J. B.; Voet, A. Carbon Black; Marcel Dekker: New York, 1976.
14. Silverstein, R. M.; Bassler, G. C.; Morril, T. C. Spectroscopic Identification of Organic Compounds; Wiley: New York, 1991.
15. Fripiat, J. J.; Uytterhoeven, J. B. J Phys Chem 1962, 66, 800.
16. Pittman, C. U.; Canaher, C. E. Polym News 1990, 15, 7.
17. MacKnight, W. J.; Taggart, W. P.; Stein, R. S. J Polym Sci Polym Symp 1974, 45, 113.
18. Mukhopadhya, K.; Tripathy, D. K.; De, S. K. J Appl Polym Sci 1993, 48, 1089.
19. Roychoudhury, A.; De, S. K. J Appl Polym Sci 1993, 50, 811.
20. Smallwood, H. M. J Appl Phys 1974, 15, 758.
21. Chakraborty, S. K.; De, S. K. Polymer 1983, 24, 1055.
22. Pal, P. K.; De, S. K. Rubber Chem Technol 1983, 56, 737.
23. Pal, P. K.; Bhowmick, A. K.; De, S. K. J Polym Mater 1982, 9, 139.
24. Pal, P. K.; De, S. K. J Appl Polym Sci 1983, 28, 3333.
25. Mathew, N. M.; Bhowmick, A. K.; Dhindaw, B. K.; De, S. K. J Mater Sci 1982, 17, 2594.